RESEARCH

Open Access

The use of cultured human alveolar basal cells to mimic honeycomb formation in idiopathic pulmonary fibrosis

Sabrina Blumer[1], Petra Khan[1], Nataliia Artysh[2,3], Linda Plappert[2], Spasenija Savic[4], Lars Knudsen[5,7], Danny Jonigk[6,7], Mark P. Kuehnel[6,7], Antje Prasse[2,3,7] and Katrin E. Hostettler[1*]

Abstract

Background Honeycomb cysts (HC) within the alveolar region are distinct histopathological features in the lungs of idiopathic pulmonary fibrosis (IPF) patients. HC are lined with a single-or stratified layer of basal cells (BC), or with a bronchiolar-like epithelium composed of basal-, ciliated- and secretory epithelial cells. By using cultured IPF patient-derived alveolar BC, we aimed to establish an in vitro- and in vivo model to mimic HC formation in IPF. We (1) optimized conditions to culture and propagate IPF patient-derived alveolar BC, (2) cultured the cells on an air liquid interface (ALI) or in a three dimensional (3D) organoid model, and (3) investigated the cells` behavior after instillation into bleomycin-challenged mice.

Methods Alveolar BC were cultured from peripheral IPF lung tissue and grown on tissue-culture treated plastic, an ALI, or in a 3D organoid model. Furthermore, cells were instilled into bleomycin-challenged NRG mice. Samples were analyzed by TaqMan RT-PCR, immunoblotting, immunocytochemistry/immunofluorescence (ICC/IF), or immunohistochemistry (IHC)/IF. Mann–Whitney tests were performed using GraphPad Prism software.

Results Cultured alveolar BC showed high expression of canonical basal cell markers (TP63, keratin (KRT)5, KRT14, KRT17), robust proliferation, and wound closure capacity. The cells could be cryopreserved and propagated for up to four passages without a significant loss of basal cell markers. When cultured on an ALI or in a 3D organoid model, alveolar BC differentiated to ciliated- and secretory epithelial cells. When instilled into bleomycin-challenged mice, human alveolar BC cells formed HC-like structures composed of human basal-, and secretory epithelial cells within the mouse parenchyma.

Conclusion IPF patient-derived alveolar BC on an ALI, in 3D organoids or after instillation into bleomycin-challenged mice form HC-like structures that closely resemble HC within the IPF lung. These models therefore represent powerful tools to study honeycomb formation, and its potential therapeutic inhibition in IPF.

Keywords Alveolar basal cells, IPF, Honeycomb cysts, Mucociliary differentiation, ALI, Organoids, Humanized mouse model

*Correspondence:
Katrin E. Hostettler
Katrin.Hostettler@usb.ch
Full list of author information is available at the end of the article

Blumer *et al. Respiratory Research*   (2024) 25:26

Page 2 of 14

Background

Idiopathic pulmonary fibrosis (IPF) is characterized by progressive destruction of the lung parenchyma and the respective irreversible loss of lung function [1]. Repetitive injuries to the alveolar epithelium and its disturbed regeneration play a critical role in disease development [2]. In the healthy lung, the alveoli are lined with alveolar epithelial cells type 1 and 2 (AT1 and 2) that facilitate gas exchange and provide the lung with the four essential surfactant proteins (SP)-A, -B, -C, and -D, of which SP-C is specifically expressed in AT2 cells [3]. After mild-to-moderate lung injury, AT2 cells regenerate the alveolar epithelium by their ability to self-renew and to differentiate into AT1 cells [3]. However, chronic lung injury in IPF results in a maladaptive repair mechanism, in which the alveolar lung parenchyma is replaced by dense fibrotic tissue and honeycomb cysts (HC). HC are lined with a single-, or stratified layer of KRT (keratin)5 + basal cells (BC) or by a stratified bronchiolar-like epithelium composed of KRT5 + basal-, acetylated tubulin (AcTub) + ciliated-, and secretory epithelial cells, mainly expressing MUC (mucin) 5B [4–9]. Although, the appearance of ectopic airway epithelial cells within the peripheral lung of IPF patients is a well described phenomena, the cells origin and functional role in disease development and progression remains largely unknown. This may partly be explained by a lack of in vitro and in vivo models that appropriately resemble HC formation in IPF.

We previously reported the fibrosis-enriched outgrowth of cells with distinct morphology from peripheral lung tissue of IPF patients [10]. Characterisation of the cells revealed their expression of canonical BC markers and close transcriptomic similarity to BC [6]. Under the previously described cell culture conditions, the cells expansion and experimental use proved difficult [6, 10, 11]. In this study, we therefore first optimized the culture of alveolar BC and then used the cells to establish in vitro and in vivo models to mimicking HC formation in IPF.

Methods

Basal cell culture

Alveolar BC were cultured from lung-explants derived from IPF patients undergoing lung transplantation as previously described [6, 11]. Briefly, lung tissue was cut into small pieces and placed into cell culture-treated plastic dishes containing the commercially available epithelial cell growth medium Cnt-PR-A. After 5–7 days the tissue pieces were removed and cells trypsinized and expanded. All experiments in this study were performed with cells between passage 1–2, except for the experiment evaluating the cell marker expression in cells between passage 0–6. For cryopreservation, confluent alveolar BC were trypsinized, re-suspended in cryo-medium (Cnt-PR-A

40%, fetal bovine serum 50%, DMSO 10%), stored in a − 80° C freezer for up to one week and then transferred to liquid nitrogen tank for long-term storage. IPF was diagnosed based on ATS/ERS guidelines [1, 12]. The local ethical committee of the University Hospital, Basel, Switzerland (EKBB05/06) and of the Hannover Medical School, Germany (2699-2015) approved the culture of human primary lung cells. Patient characteristics can be found in Additional file 2: Table S1. All materials used in this study are listed in Additional file 2: Table S2.

TaqMan RT-PCR, immunoblotting, immunohistochemistry, immunocytochemistry, and immunofluorescence

TaqMan® RT-PCR, immunoblotting, immunocytochemistry (ICC)/immunofluorescence (IF), immunohistochemistry (IHC)/IF or hematoxylin and eosin (H&E) stainings were performed as previously described [6, 11, 13]. TaqMan PCR results are expressed as − ΔCt values (− (target-GAPDH)). Missing − ΔCt values (because the target genes was expressed at too low level to be detected after 40 cycles) were arbitrarily set to -20. Details for primers and antibodies are listed in Additional file 2: Table S2. Immunoblots were cropped to improve the visibility of the bands of interest. The corresponding full-length immunoblots are provided in Additional file 1: Fig. S1.

Image acquisition and image processing

Lung tissue slides from non-fibrotic control- and IPF patients (see patient characteristics in Additional file 2: Table S1) were acquired as followed: Images of lung tissue were captured with Photometrics Prime 95B camera using a Nikon Plan Apo 20× objective (0.75 NA) at Nikon Ti2-E widefield microscope and stitched together to one large image (2555×2555 µm, pixel size 0.55 µm/pixel) using Nikon NIS Elements 4.21 software. Fluorophores (Alexa488, Alexa555, Alexa647) with 488 nm, 555 nm, 647 nm lasers, respectively and a band pass emission filter (LED-DA/FI/TR/Cy5/Cy/-5x-A) were used. A total number of six large images of each IPF- or non-fibrotic control patient-derived lung tissue were analyzed. All acquired images were stored on the client–server platform Omero (Omero.insight 5.5.17 and Omero.web 5.9.1) for managing microscope images.

IF images were analyzed with Qupath version 0.3.4 (an open-source software for bioimage analysis) [14] using a script for each target protein including nuclei segmentation, pixel- and object classification. StarDist 2D (model: *dsb2018_heavy_augment.pb*), a deep-learning based-method of nucleus detection were used for IF images [15]. All parameters used for cell detection in Qupath are listed in Table 1. Following nuclei segmentation, the data were further classified for each marker (cytosol,

Blumer *et al. Respiratory Research*   (2024) 25:26

Page 3 of 14

Table 1 Parameters used in Qupath script

Parameters	Values
Probability (detection) threshold	0.5
Selected detection channel	DAPI
Percentile normalization	1, 99
Resolution for detection (pixel size)	0.275
Cell expansion	1.0
Cell constrains scale	1.5
Probability	True
Intensity threshold parameters (localization)	
SP-C (cytosol)	800
KRT17 (cytosol)	400
KRT5 (cytosol)	400
KRT14 (cytosol)	700
p63 (nucleus)	1000
AcTub (membrane)	400
SCGB1A1 (cytosol)	400
MUC5AC (cytosol)	300
MUC5B (cytosol)	300
MMP7 (cytosol)	600

nucleus or membrane depending on the target labeling) and applied to all datasets. For each marker, thresholds were set visually and mean intensity was assessed to quantify positive cells in lung tissue. Data is presented as mean ± SEM.

Air liquid interface culture

For air liquid interface culture (ALI), alveolar BC were seeded on 12 mm transwell inserts (apical chamber) in a 12-well plate (basal chamber) and grown to confluence by adding Cnt-PR-A to the basal and apical chamber. To initiate differentiation, Cnt-PR-A medium was aspirated from both chambers. PneumaCult-ALI maintenance medium was prepared according to the manufacturer's instructions and added to the basal chamber only. Medium in the basal chamber was changed every 2–3 days for a total of 23 days. The cells on the transwell membranes were either lysed for RNA expression analysis or fixed in 4% paraformaldehyde (PFA) and analyzed by ICC/IF. Alternatively, the cells were fixed in 4% PFA for 15 min at RT, embedded in Tissue-Tek® O.C.T. compound after 30% and 15% sucrose incubation and snap frozen in 2-methylbutan with liquid nitrogen. Frozen sections were cut into 7 µm on a cryostat and analyzed by ICC/IF.

3D organoid culture

Cultured alveolar BC were trypsinized and resuspended in 40 µl ice-cold Matrigel at a density of 500 cells/µl. Droplets were placed in a pre-warmed 24-well

suspension plate and incubated for 20 min (37 °C, 5% CO_2). Differentiation media formulations were slightly modified from a previously described protocol [16]: Basic differentiation media (bDM) consists of IMDM-Ham`s F12 (3:1 vol/vol) with B 27 (with retinoic acid) supplement (1%), N 2 supplement (0.5%), BSA (0.05%), antibiotic–antimycotic 1 ×, glutamax 1 ×, ascorbic acid (50 µg/ml) and monothioglycerol (4.5×10^{-4} M). Complete differentiation medium (cDM) consists of bDM supplemented with FGF-2 (250 ng/ml), FGF-10 (100 ng/ml), EGF (5 ng/ml), dexamethasone (50 nM), 8-Bromo-cAMP (0.1 mM) IBMX (0.1 mM), and A83-01 (TGF-ß inhibitor, 1 µM). For the first 7 days, a mixture of epithelial cell growth medium (Cnt-PR-A) and cDM (1:1) with ROCK inhibitor (Y-27632 dihydrochloride, 10 µM) was added to the wells. The medium was then changed to cDM and incubated for another 14 days. cDM was exchanged once after 7 days. On day 20 droplets with organoids were imaged at 10× with a z-stack (every 50 µm) and stitched together by Nikon Ti2-E widefield microscope. The diameter and number of organoids per mm^3 with a diameter > 50 µm as well as the percentage of organoids with polarized lumen was determined by using Fiji software version 2.9.0 [17]. On day 21 the Matrigel was digested with Dispase II (2 mg/ml) for 20min at 37°C and organoids were fixed in 4% PFA for 30 min, embedded in pre-heated histogel, polymerized for 1 h at RT and stored in 50% ethanol for up to 1 week. Organoids were then dehydrated using ethanol series (50%, 70%, 95%, 100%) followed by Xylene incubation and then embedded in paraffin. Paraffin blocks were cut on a microtome into 4 µm sections and analysed by ICC/IF. For ICC/IF image quantification, a selection of organoids (n = 10) across each IPF patient (n = 4) was captured at 40× using a Nikon Ti2-E widefield microscope. Automated counting of single-color images (each channel separately) for target proteins of each organoid was performed in FIJI. Alternatively, organoids were lysed for RNA expression analysis.

Proliferation assay

Alveolar BC were seeded into two wells of a 24-well plate. When the cells reached about 70% confluence, one of the wells was stained with live cell stain NucBlue, imaged at 4× using a Nikon Ti2-E widefield microscope and the cells counted by using the general analysis NIS software version 4.2.1 (time point 0). The same procedure was repeated with the second well after 48 h.

Epithelial wound repair assay

Alveolar BC were seeded into 12-well culture plates and grown to confluence. The cell layer was mechanically wounded by using a pipette tip. Wound closure was monitored by using a Nikon Ti2 2.3.PO widefield

time lapse microscope and calculated by using a Fiji plugin wound healing size tool [18].

Intratracheal administration of human alveolar BC into bleomycin-challenged mice

All mouse procedures were conducted at the Hannover Medical School, Germany in accordance with the German law for animal protection and the European Directive 2010/63/EU and were approved by the Lower Saxony State Office for Consumer Protection and Food Safety in Oldenburg/Germany (LAVES); AZ: 33.12-42502-04-15/1896 and AZ: 33.19-42502-04-15/2017), AZ:33.12-42502-04-17/2612). Human alveolar BC were cultured as described earlier and some of the cells were transduced with a lentiviral vector (kindly provided by Dr. Axel Schambach, Hannover Medical School) for firefly-luciferase and enhanced green fluorescence protein (eGFP) as previously described [19]. A total of nine NRG mice received bleomycin at a dose of 1.2 mg/kg intratracheally at day 0. Three days later, three mice were intratracheally injected with human alveolar BC, and three mice with vector-transduced human alveolar BC (in both conditions: 0.3×10^5 cells per mouse). For in vivo imaging of firefly-luciferase activity in vector-transduced human alveolar BC, the respective mice were injected subcutaneously with XenoLight D-Luciferin-K + Salt Bioluminescent Substrate (150 mg/kg) on day 1, 8 and 15. Bioluminescence was subsequently measured by an IVIS Lumina II and data analyzed using LivingImage 4.5 as previously described [19]. At day 21 mouse lungs were harvested and embedded in paraffin for IHC/IF analysis.

Statistics

Experiments were performed in alveolar BC derived from multiple different IPF patients as indicated by the n-numbers for each individual experiment. Statistical analysis was performed using GraphPad Prism software version 9.1.1. A Mann–Whitney test was applied to determine p values, and the data are presented as mean ± SEM. All p values < 0.05 were considered as statistically significant.

Results

The alveolar lung parenchyma is replaced by dense fibrotic tissue and HC in IPF lung tissue

Compared to the normal alveolar lung parenchyma with some peripheral bronchioles in close proximity to pulmonary arteries in non-fibrotic lung tissue of control patients (n = 4), the alveolar lung parenchyma in IPF patients is destroyed and replaced by dense fibrosis with multiple HC (n = 4) (Fig. 1A). IPF lung tissue (n = 4) displayed a reduced number of SP-C + AT2 cells when compared to non-fibrotic lung tissue of control patients (n = 4) (Fig. 1B, D). Cells positive for the canonical basal cell marker KRT17, KRT5 and tumor protein 63 (p63), or secretory (secretoglobin family 1A member 1 (SCGB1A1)+, MUC5B+)- or ciliated (AcTub+) epithelial cells were detected within distal bronchioles of non-fibrotic controls tissue and within HC in IPF tissue (Fig. 1B). Overall numbers of KRT17-, KRT5-, p63-, SCGB1A1-, MUC5B-, or AcTub-expressing epithelial cells was significantly higher in IPF when compared to control tissue (Fig. 1C, D). KRT14 was only expressed in a fraction of cells within IPF, but not in control lung tissue (Fig. 1C, D). MUC5AC + cells were absent in the alveolar epithelium of control tissue and only detected in small numbers in IPF lungs (Fig. 1C, D). Matrix metalloprotease (MMP)7, an established biomarker for IPF [20], was only detected in IPF, but not in control lung tissue (Fig. 1C, D).

Cultured alveolar BC express high levels of basal cell markers, and show a robust proliferation and wound healing capacity

Peripheral IPF lung tissue was cut in small pieces and placed in cell culture dishes containing an epithelial cell specific growth medium (Cnt-PR-A) as illustrated in Fig. 2A. Outgrown alveolar BC expressed high levels of TP63 (gene name of the p63 protein), KRT5, KRT14, and KRT17 on the RNA (Fig. 2B) and protein (Fig. 2C) level. RNA of the secretory epithelial cell marker SCGB1A1 or mesenchymal marker CDH2 was either not expressed or expressed at very low levels (Fig. 2B). SCGB1A1 or CDH2 proteins were absent in cultured cells (Fig. 2C).

Cultured alveolar BC displayed robust proliferation, shown by a significant increase in cell numbers between

(See figure on next page.)

Fig. 1 Ectopic epithelial cells in peripheral IPF lung tissue. Representative images showing Hematoxylin and Eosin (H&E) stainings in control (n = 4) and IPF (n = 4) lung tissue (**A**). Representative IHC/IF images of control (n = 4) and IPF (n = 4) lung tissue incubated with antibodies detecting SP-C (**B**), MMP7, or basal (KRT5, KRT17, KRT14, p63)-, ciliated (AcTub)-, or secretory (SCGB1A1, MUC5AC, MUC5B) epithelial cell markers (**C**). White squares indicate regions imaged at higher magnification shown in the top right corner of the image (**B**, **C**). IHC/IF image quantifications of cells expressing specific markers within control (n = 4) and IPF (n = 4) tissue (**D**). Dots within the bar charts represent individual data points generated by analysis of six images of control (n = 4) and IPF (n = 4) lung tissue. Data are expressed as mean ± SEM (Mann–Whitney test, **** indicates p < 0.0001)
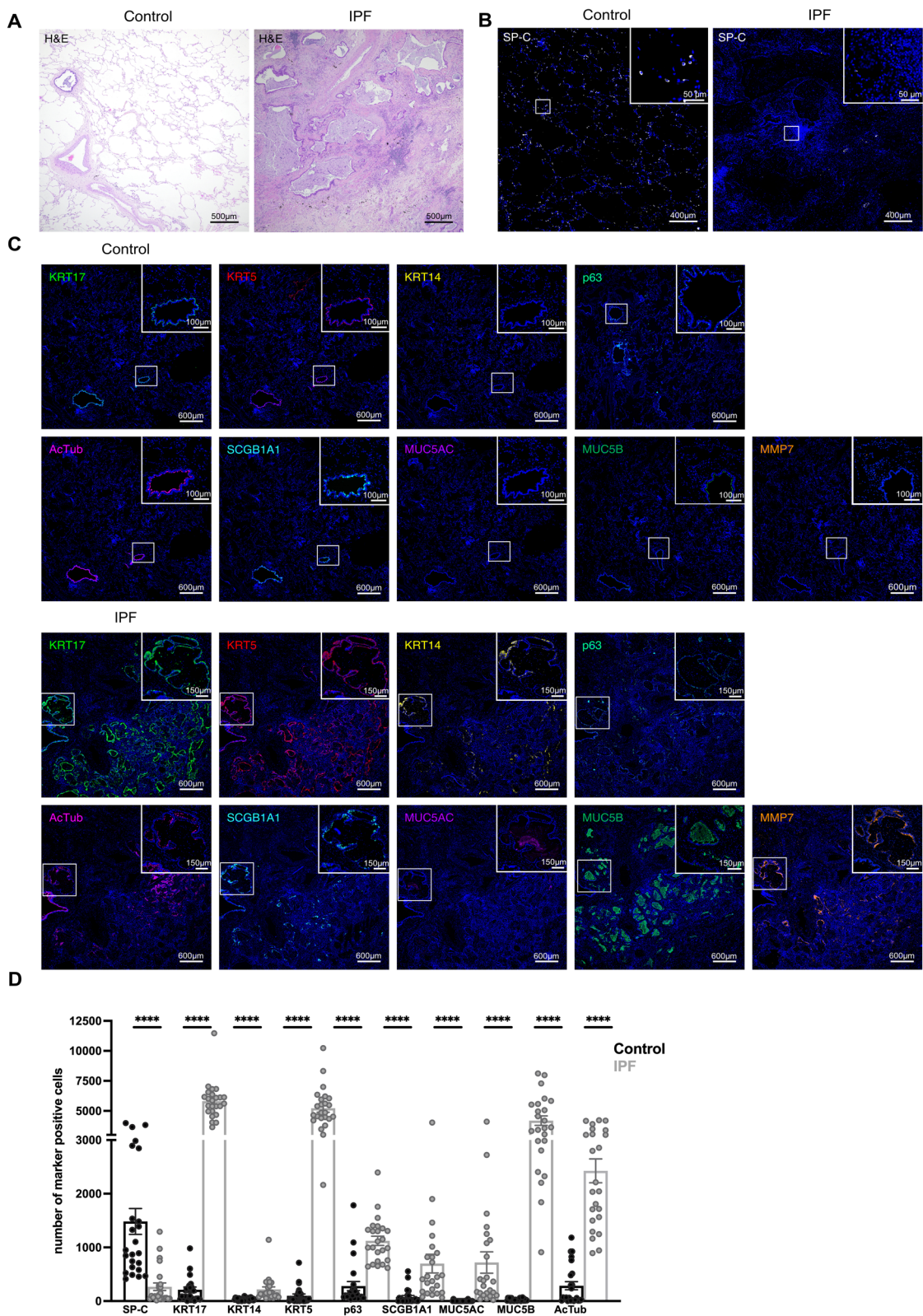
Fig. 1 (See legend on previous page.)
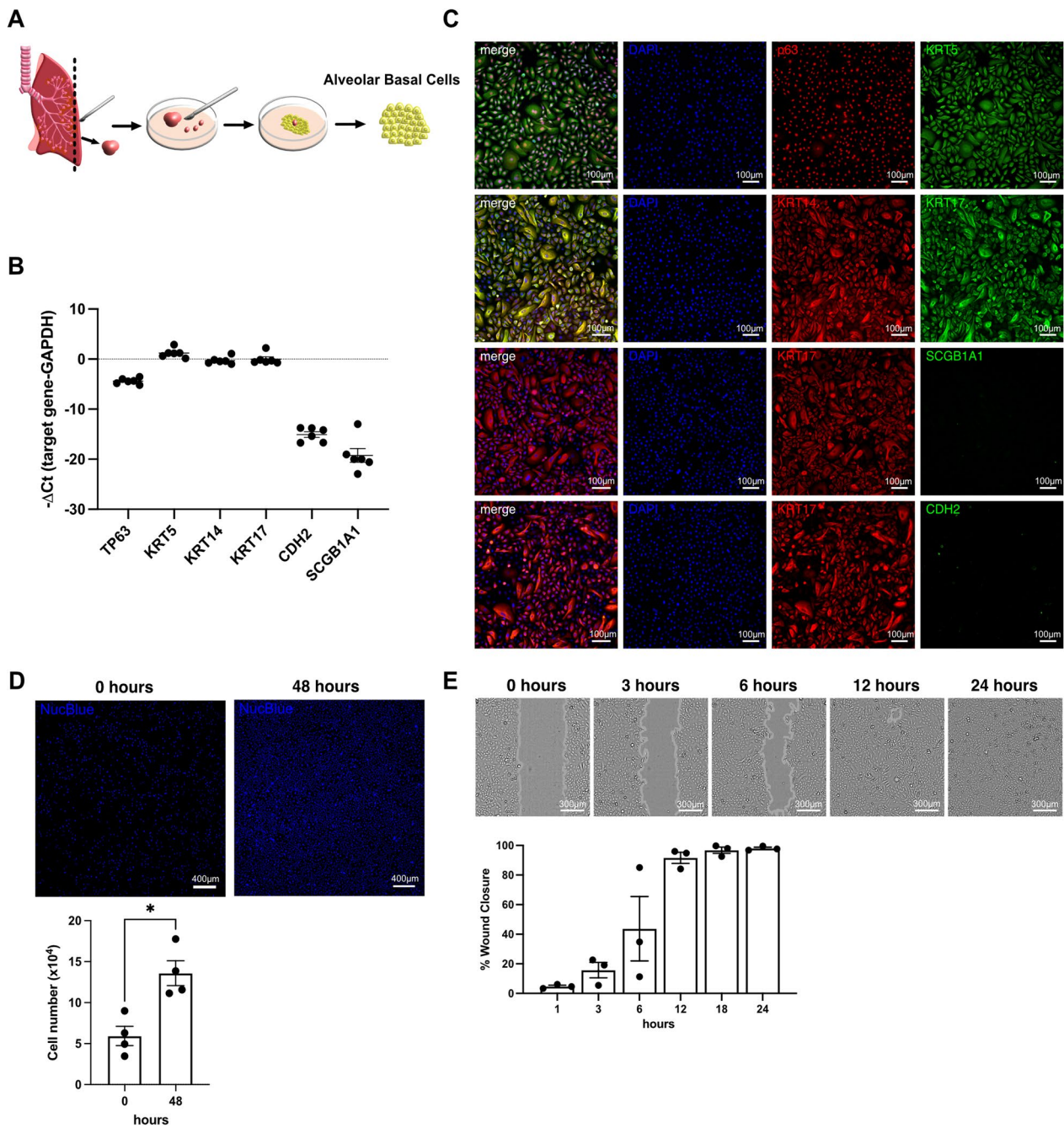
Fig. 2 Characteristics of cultured alveolar basal cells. Illustration of alveolar BC culture (**A**). Experiments presented in this figure were performed in alveolar BC from 3 to 6 different IPF patients (n-number). RNA expression levels (− ΔCt) of TP63, KRT5, KRT14, KRT17, CDH2 and SCGB1A1 in alveolar BC (n=6). Data are expressed as mean±SEM (**B**). Representative single- or merged ICC/IF images of alveolar BC (n=4) incubated with antibodies detecting KRT5, p63, KRT17, KRT14, SCGB1A1, or CDH2. Nuclei were counter-stained with DAPI. Automated cell counts of alveolar BC at 0 and 48 h (n=4) (D). Alveolar BC wound closure between 0 and 24 h (n=3) (**E**). Dots within the bar charts represent datapoints generated for alveolar BC from each patient. Data are expressed as mean±SEM (Mann–Whitney test, * indicates p < 0.05)

Blumer *et al. Respiratory Research*   (2024) 25:26

Page 7 of 14

0 to 48 h (Fig. 2D) and wound healing capacity by closing a mechanically set scratch after 12 h (Fig. 2E).

Alveolar BC can be propagated for up to four passages and cryopreserved without significant loss of basal cell markers

Confluent alveolar BC were trypsinized and split at a ratio of 1 to 2 for up to six passages or were cryopreserved in cryo-medium. Between passage 0–4, no reduction in the expression of basal cell marker KRT5 and TP63 or that of the canonical epithelial cell marker CDH1 was detected on the RNA (Fig. 3A) or protein level (Fig. 3B). When comparing to earlier passages, a slight decrease in KRT5 and TP63 expression was observed on the RNA level at passage 6, which reached significance for TP63 (Fig. 3A). On the protein level, KRT5 and TP63 were significantly reduced at passage 5 (Fig. 3B, C). The mesenchymal marker CDH2 was detected at very low levels on the RNA level (Ct values > 30) (Fig. 3A) and was absent on the protein

level in cells between passage 1–5 (Fig. 3B). Similarly, alveolar BC before (fresh) and after cryopreservation (thawed) did not show any significant changes in KRT5, TP63, CDH1, or CDH2 RNA expression (Fig. 3D).
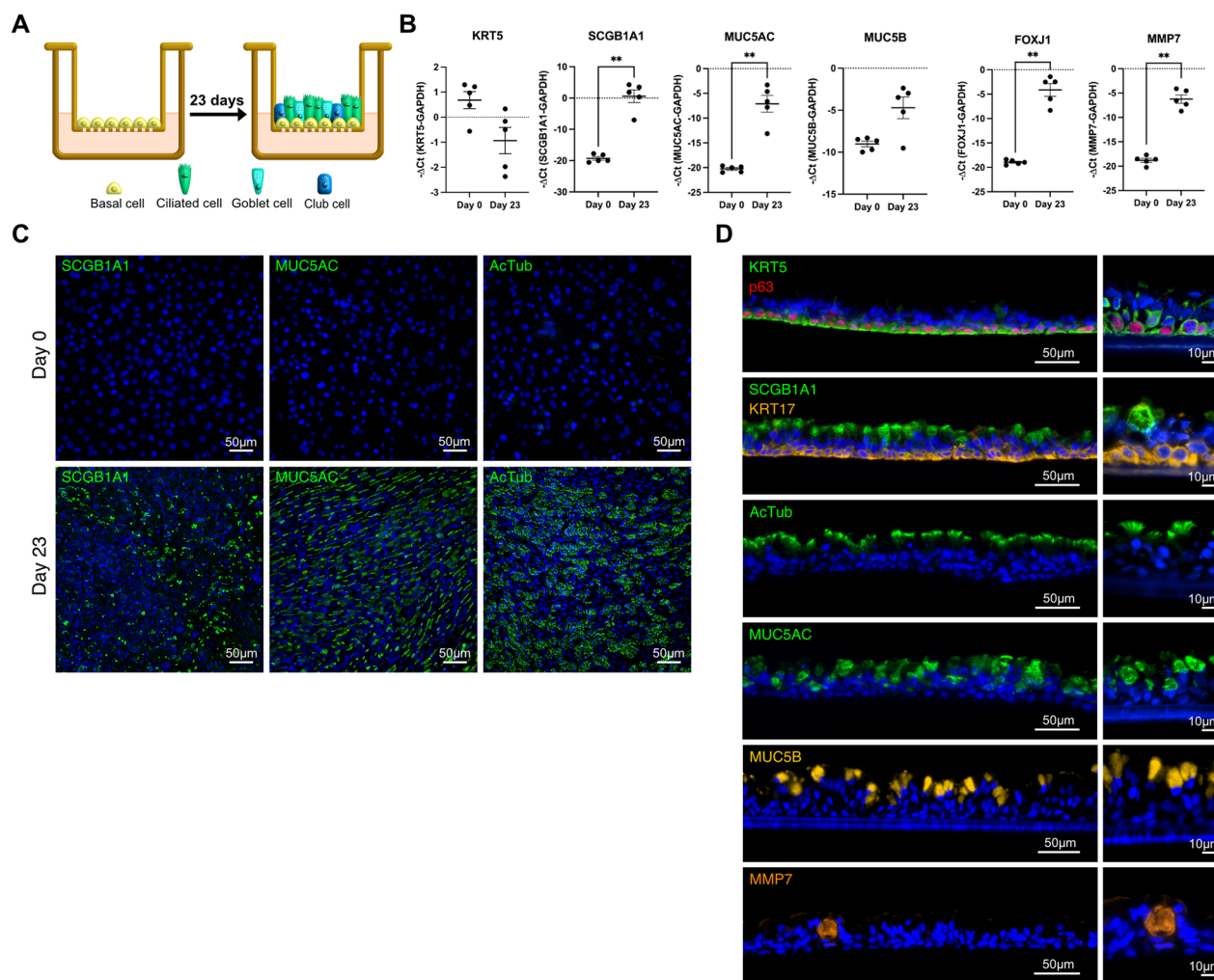
Alveolar BC differentiate towards ciliated- and secretory epithelial cells when cultured on an ALI or in a 3D organoid model

Illustration of mucociliary differentiation of alveolar BC cultured on an ALI platform for 23 days (Fig. 4A). At day 0, RNA expression of the basal cell marker KRT5 is high and that of MMP7, secretory (SCGB1A1, MUC5AC, MUC5B)- or ciliated (FOXJ1) epithelial cell markers are absent or expressed at low levels (Fig. 4B). After 23 days of ALI culture, RNA of MMP7 and all secretory- and ciliated epithelial cell marker are up-regulated and that of KRT5 down-regulated (Fig. 4B). Similarly, SCGB1A1-, MUC5AC-, and AcTub proteins are absent in cells at day 0 and abundantly present in cells at day 23 (Fig. 4C). Immunofluorescence stainings of transwell
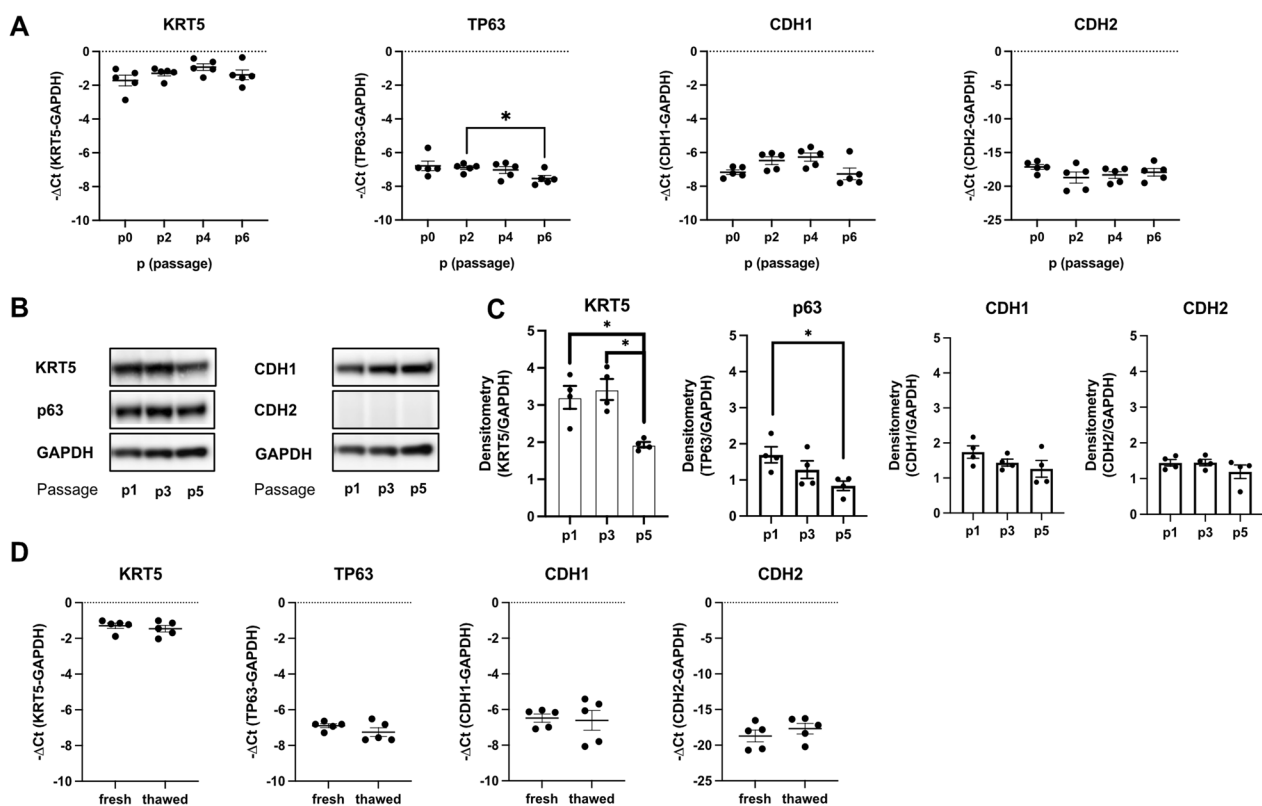
Fig. 3 Alveolar basal cell marker expression is stable over several passages and after cryopreservation. Experiments presented in this figure were performed in alveolar BC from 4–5 different IPF patients (n-number). RNA expression levels (− ΔCt) of KRT5, TP63, CDH1 or CDH2 in alveolar BC (n = 5) at passage (p) 0, 2, 4, and 6 (**A**). Representative immunoblots (cropped) showing the protein expression of KRT5, p63, CDH1, CDH2 or GAPDH in alveolar BC (n = 4) at p1, p3, and p5 (**B**) and their densitometry analysis relative to the house keeping gene GAPDH. The corresponding uncropped immunoblots are provided in figure S1. Dots within the bar charts represent datapoints generated for alveolar BC from each patient (**C**). RNA expression levels (− ΔCt) of KRT5, TP63, CDH1 or CDH2 in alveolar BC (n = 5), before (fresh) and after (thawed) cryopreservation (D). Data are expressed as mean ± SEM (Mann–Whitney test, * indicates p < 0.05)

Blumer *et al. Respiratory Research*   (2024) 25:26

Page 8 of 14

Fig. 4 Alveolar basal cells cultured on an ALI differentiate to secretory- and ciliated epithelial cells. Illustration of alveolar BC ALI culture (**A**). Experiments presented in this figure were performed in alveolar BC from 3–5 different IPF patients (n-number). RNA expression levels (− ΔCt) of KRT5, SCGB1A1, MUC5AC, MUC5B, FOXJ1, or MMP7 in alveolar BC (n = 5) cultured on an ALI on day 0 and day 23. Data are expressed as mean ± SEM (Mann–Whitney test, ** indicates p < 0.01) (**B**). Representative ICC/IF images of ALI cultured alveolar BC (n = 2) incubated with antibodies detecting SCGB1A1, MUC5AC, or AcTub at day 0 and day 23 (**C**). Representative images of ALI culture cryosections (n = 3–4) incubated with antibodies detecting KRT5, KRT17, p63, SCGB1A1, MUC5AC, AcTub, MUC5B or MMP7 at day 23 (**D**). Nuclei were counter-stained with DAPI (**C**, **D**)

membrane cryosections show alveolar BC differentiation into a stratified epithelial cell layer with KRT5+/KRT17+/p63+basal cells at the basal region and secretory (SCGB1A1+, MUC5AC+, MUC5B+, MMP7+)-, and ciliated (AcTub+) epithelial cells at the apical region (Fig. 4D).

Alveolar BC were embedded in Matrigel and cultured for 21 days (Fig. 5A). Cells expand in numbers and start to self-assemble into clusters at day 2. Organoids (>50 μm diameter) first formed after 7 days and continued to grow over a period of 21 days (Fig. 5B). After 20 days, 43–100 organoids/mm^3 with a diameter of 50-280 μm were formed (Fig. 5C). Cells within

organoids expressed KRT17-, KRT5-, TP63-, SCGB1A1-, MUC5AC-, MUC5B-, FOXJ1-, and MMP7 RNA (Fig. 5D). Furthermore, cells showed positive IF signals for KRT17-, KRT5-, p63-, AcTub-, MUC5AC-, MUC5B-, and MMP7 as presented in Fig. 5E and quantified in Fig. 5F. Polarized lumen were present in approximately 40% of the organoids after 21 days, with BC (KRT5+, KRT17+, p63+) mainly located at the outer layer, and ciliated (AcTub+)-, secretory (SCGB1A1+, MUC5AC+, MUC5B+)-, or MMP7+epithelial cells at the luminal site of the organoids. Similar to HC within the IPF lung (Fig. 1C), the lumen of the organoids were filled with MUC5B + or MUC5AC + mucus (Fig. 5G).

Blumer *et al. Respiratory Research*   (2024) 25:26

Page 9 of 14
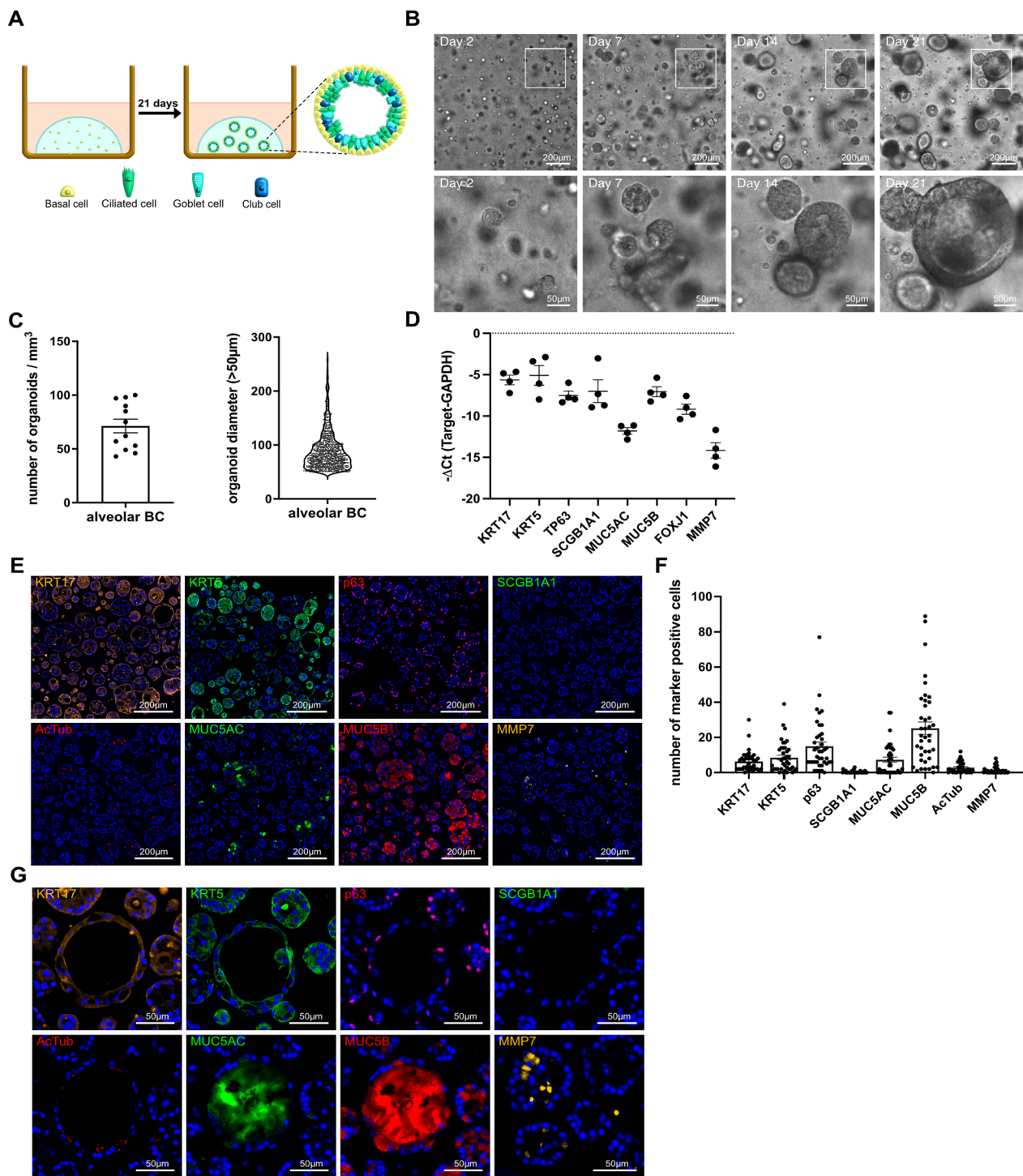
Fig. 5 Alveolar basal cells form organoids and differentiate to secretory- and ciliated epithelial cells. Alveolar BC were resuspended in Matrigel and cultured for 21 days as illustrated (**A**). Experiments presented in this figure were all performed in alveolar BC from 4 IPF patients (n-number). Representative phase contrast images of organoid formation at day 2, 7, 14, and 21 (**B**). Graphs, showing the number of organoids/mm³ (mean ± SEM) and the distribution of their diameters > 50 µm (violin plot) of three selected regions (1 mm³) per IPF patient (n = 4) after 20 days (**C**). RNA expression levels (− ΔCt) of KRT17, KRT5, TP63, SCGB1A1, MUC5AC, MUC5B, FOXJ1, or MMP7 in organoids after 21 days. Data are presented as mean ± SEM (**D**). Representative ICC/IF images of organoids incubated with antibodies detecting KRT17, KRT5, p63, SCGB1A1, AcTub, MUC5AC, MUC5B, or MMP7 (**E**), and their quantification (mean ± SEM). Dots within the bar charts represent individual data points generated by analysis of 10 organoids per IPF patient (n = 4) (**F**). Representative ICC/IF images of organoids incubated with antibodies detecting KRT17, KRT5, p63, SCGB1A1, AcTub, MUC5AC, MUC5B, or MMP7 (**G**). Nuclei were counter-stained with DAPI (**G**)

Human alveolar BC engraft and differentiate in lung tissue of bleomycin-challenged mice

Mice were intratracheally challenged with a low dose of bleomycin for three days and were subsequently intratracheally injected with human alveolar BC or human alveolar BC transduced with a luciferase and GFP encoding vector. Mice were sacrificed after 21 days (Fig. 6A). Luciferase expression in mice injected with cells carrying a luciferase encoding vector, increased over time, suggesting pulmonary engraftment and proliferation of human alveolar BC (Fig. 6B, C). H&E stainings showed mild fibrotic changes in lung tissue of bleomycin-challenged mice (Fig. 6D). In lung tissue of mice injected with human alveolar BC, we observed extensive accumulation of cell with squamous morphology (Fig. 6D). Human BC invaded the alveolar space and partly destroyed alveolar septa (Fig. 6E). Cells stained positive for the human-specific protein HNA, confirming their human origin (Fig. 6F). IF stainings for basal- (KRT5, KRT17), secretory- (MUC5AC, MUC5B, SCGB1A1), or ciliated (AcTub) epithelial cell markers revealed that the human BC maintain their basal cell identity and differentiated towards secretory MUC5AC+, MUC5B+, SCGB1A1+ epithelial cells (Fig. 6F).

Discussion

In IPF, the alveolar lung parenchyma is replaced by dense fibrotic tissue and HC that are lined with a bronchiolar-like epithelium [8]. In line with this, we here reported reduced numbers of SP-C+AT2 cells, accompanied with the appearance of ectopic airway epithelial cells including basal-, ciliated-, and secretory epithelial cells within peripheral IPF lung tissue. Our findings are in agreement with several recent studies, showing dramatic changes in epithelial cell subtypes and the emergence of airway epithelial- and fibrosis-specific intermediate cell types, which mainly localize within HC in the IPF lung [4, 5, 9, 21–26]. Although, the appearance of airway epithelial cells in the peripheral IPF lung is a widely accepted phenomenon, the cells origin remains elusive: Migration of airway epithelial cells into the alveolar space after injury [27], trans-differentiation of resident AT2 cells into alveolar BC [22, 23] or the occurrence of both mechanisms

in parallel have been proposed [25]. In addition, the cells functional role in disease development and progression is largely under-investigated. In animal models, basal-like cells helped to regenerate the injured alveolar epithelium [28, 29], whereas alveolar BC in the lung of IPF patients were associated with increased mortality and pathological HC formation [4, 19]. By using IPF patient-derived alveolar BC, we here established in vitro and in vivo models that closely resemble HC formation in IPF. The use of such disease models will greatly contribute to a better understanding of the role and function of alveolar BC in IPF.
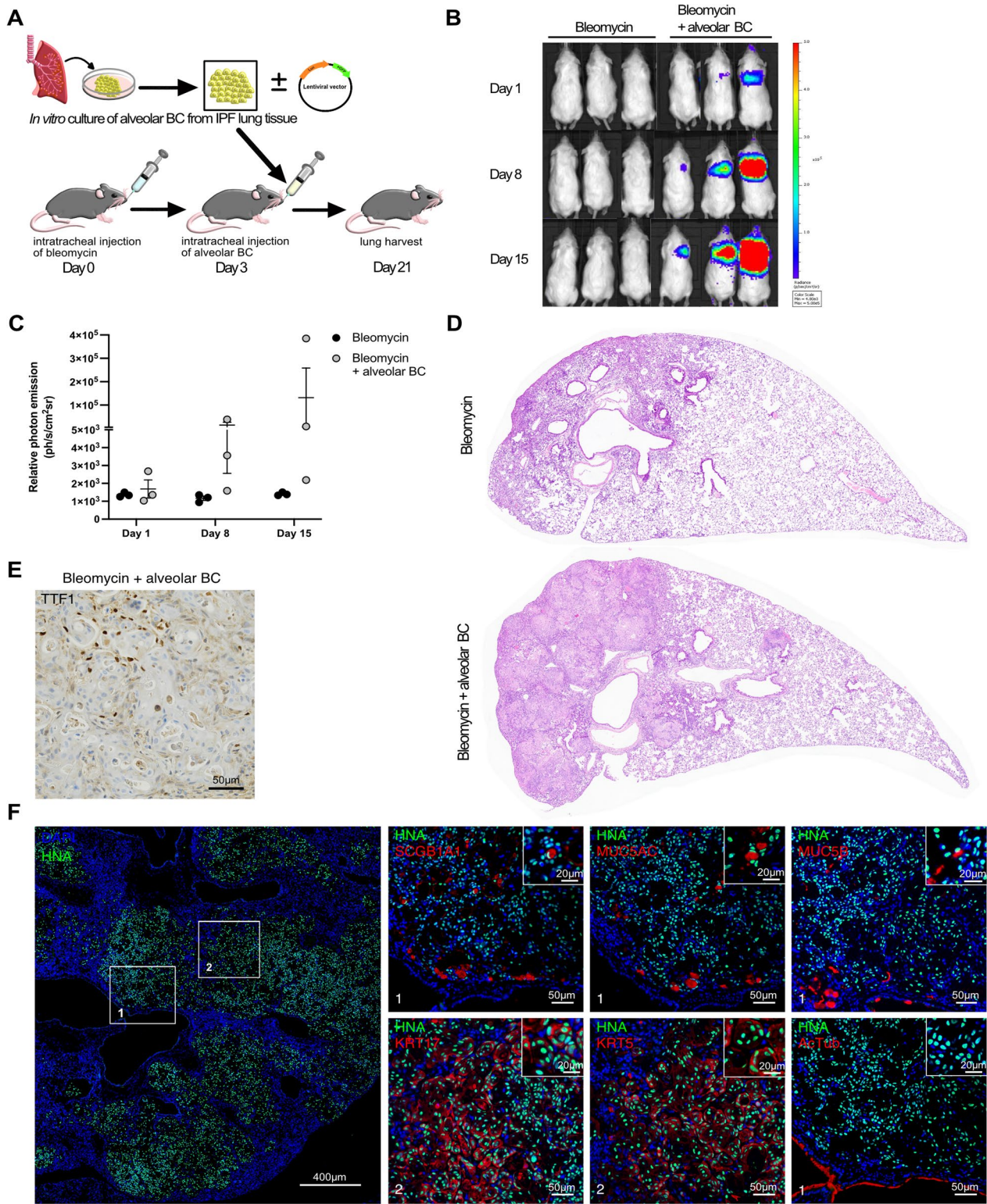
We previously described the fibrosis-enriched outgrowth and *the vitro* culture of alveolar BC [6, 10, 11]. Under the previously described culture conditions, alveolar BC underwent growth arrest after a short culture period and spontaneously differentiated towards secretory- or aberrant basaloid-like cells, making long-term expansion and experimental use of the cells difficult [6, 11]. We previously cultured alveolar BC in DMEM growth medium [6, 11], which contains high concentrations of calcium and likely lacks factors essential for the growth of epithelial cells. High calcium concentrations were shown to inhibit growth and to promote differentiation of epithelial cells [30, 31], likely explaining the cells insufficient proliferation and spontaneous differentiation in DMEM growth medium [6, 11]. In this study, we replaced DMEM growth medium with the commercially available Cnt-PR-A medium, which was specifically developed to support growth and to inhibit differentiation of primary epithelial cells. Indeed, when cultured in Cnt-PR-A, alveolar BC expressed high levels of the canonical basal cell markers KRT5, KRT17, KRT14, and p63 and showed the capacity for robust proliferation and wound healing. Furthermore, spontaneous differentiation of alveolar BC was not observed under the optimized culture conditions and we were able to cryopreserve and expand the cells for several passages without loss of BC-specific markers.

We next aimed to establish in vitro models that closely resemble HC in the IPF lung, by using IPF patient-derived alveolar BC. IF stainings of peripheral IPF lung tissue, confirmed the presence of KRT5+/KRT17+basal-,

(See figure on next page.)

Fig. 6 Human alveolar basal cells form HC-like structures in bleomycin-challenged mouse lungs. NRG mice were treated with bleomycin (n=3), or bleomycin+human alveolar BC carrying a luciferase encoding vector (n=3), or bleomycin+human alveolar BC (n=3) as illustrated (**A**). Luciferase expression in mice treated with bleomycin or bleomycin+human alveolar BC carrying a luciferase encoding vector (**B**) and the corresponding bioluminescence measurements (**C**) at day 1, 8, and 15. Representative images of H&E stainings in mice treated with bleomycin or bleomycin+human alveolar BC (**D**). Representative IHC image of TTF-1 in mice treated with bleomycin+human alveolar BC (**E**). Representative IHC/IF images of mouse lung tissue (mice treated with bleomycin+human alveolar BC) incubated with antibodies detecting human-specific HNA with or without SCGB1A1, MUC5AC, MUC5B, KRT17, KRT5, or AcTub. Nuclei were counter-stained with DAPI. White squares (1, and 2) indicate regions imaged at higher magnification (**F**)

Fig. 6 (See legend on previous page.)

Blumer *et al. Respiratory Research*   (2024) 25:26

Page 12 of 14

AcTub+ciliated- and SCGB1A1+, MUC5B+ and MUC5AC+secretory, and MMP7+epithelial cells within HC in the IPF lung. In accordance with other studies [5, 9], KRT5+/KRT17+, and MUC5B+cells were the most prevalent cell types, whereas MUC5AC+cells were detected only in small numbers. MMP7+cells were detected in IPF, but not in non-fibrotic peripheral lung tissue as previously reported [32, 33]. It was previously shown that airway BC differentiate to ciliated- and secretory epithelial cells when cultured on an ALI platform [34], whereas submerged culture of the cells prevented ciliary differentiation [35]. We therefore cultured IPF-derived alveolar BC on an ALI platform, which induced their differentiation to ciliated- and secretory epithelial cells. In addition, we embedded alveolar BC into Matrigel in which they formed 3D organoids. Similar to our observations in ALI culture, alveolar BC-derived organoids were composed of basal-, ciliated-, and secretory epithelial cells. The cellular composition of alveolar BC-derived organoids closely resembled that of HC in vivo, with KRT5+/KRT17+basal− and MUC5B+ cells being the most prevalent cell types. MMP7 was absent in non-differentiating alveolar BC, and induced when cultured on an ALI platform, or in a 3D organoid model. MMP7 is expressed by aberrant basaloid cells and by secretory epithelial cells as well as other airway epithelial cells [21, 22, 32], suggesting that transitional BC and/or their progeny may be the source of MMP7 in our in vitro models. However, the exact cell type producing MMP7 in our in vitro models still needs to be determined in future studies.

Next, we examined alveolar BC behaviour after instillation into bleomycin-challenged mice. It was previously shown that airway-derived BC instilled in bleomycin-challenged mice, form HC-like structures within mouse lung tissue [19]. Using the same animal model and protocol [19], we here show that IPF patient-derived alveolar BC engraft and proliferate in the lungs of bleomycin-challenged mice. Furthermore, we showed that human alveolar BC differentiate to secretory epithelial cells within mouse tissue, suggesting a beginning formation of HC. In our study, the human alveolar BC-driven HC formation within mouse lungs was less pronounced as described previously [19]. A possible explanation for these differences may be that BC in our study were cultured from the lung parenchyma, whereas Jaeger et al. obtained BC from the airways via bronchial brushings [19], suggesting that BC derived from different locations within the lung may display different characteristics and functions. Despite some differences, we believe that the here and previously described humanized mouse model [19] serves as a valuable model to study basal cell-driven HC formation in vivo.

Conclusions

In summary, the here described in vitro and in vivo models represent powerful tools to study HC formation in IPF. A limitation of this study may be a seemingly missing control BC population, cultured from non-fibrotic peripheral lung tissue. However, we previously showed that by using our standardized cell culture protocol, BC readily grew from fibrotic, but rarely from non-fibrotic peripheral lung tissue, which makes it difficult to provide a valid control basal cell population [10]. Although, our models may not fully reflect the in vivo situation of IPF HC, they appear superior to previously used models [19, 34] as BC, used in this study, 1) are IPF patient-derived and 2) were isolated from fibrotic IPF parenchyma, and not from the airways. Using cells from patient-derived tissue and from the region of interest seems important as it was shown that cells maintain disease- and region-specific characteristics when cultured in vitro [36, 37]. Although our current study does not provide new insights into the origin or function of alveolar BC in IPF, the use of the here presented models in future studies will greatly enhance our knowledge about the role of alveolar BC in HC formation and its potential pharmacological inhibition in IPF.

Supplementary Information

The online version contains supplementary material available at https://doi.org/10.1186/s12931-024-02666-9.

> **Additional file 1: Figure S1**. Full-length immunoblots.
>
> **Additional file 2: Table S1**. Patient characteristics. **Table S2**. Materials used in this study.

Author contributions

SB: Cell culture of human primary lung cells, ALI and organoid processing, ICC/IF, IHC/IF, image acquisition and image quantification in cultured cells, human IPF- and mouse tissue slides, immunoblotting, PCR, proliferation assay, scratch assay, data analysis and interpretation, revision and editing of the manuscript; PK: Conception and design of the study, cell culture of human primary lung cells, PCR, data analysis and interpretation, writing the manuscript; NA: bleomycin-mouse model, data analysis and interpretation, revision and editing of the manuscript for important intellectual content; LP: bleomycin-mouse model, data analysis and interpretation, revision and editing of the manuscript for important intellectual content; SS: Paraffin embedding, cutting, and H&E stainings of non-fibrotic control- and IPF lung tissue, interpretation of stainings performed on human IPF- and mouse lung tissue slides, revision and editing of the manuscript for important intellectual content; LK: Provided samples of IPF lung explants, revision and editing of the manuscript. DJ: Provided samples of IPF lung explants, revision and editing of the manuscript. MK: Provided samples of IPF lung explants, revision and editing of the manuscript; AP: bleomycin-mouse model, data analysis and interpretation, revision and editing of the manuscript for important intellectual content; KEH: Conception and design of the study, data analysis and interpretation, revision and editing of the manuscript for important intellectual content.

Availability of data and materials

The datasets generated and analysed during the current study are available from the corresponding author on reasonable request. Data revealing confidential patient information cannot be shared with the research community.

Declarations

Ethics approval and consent to participate

The local ethical committee of the University Hospital, Basel, Switzerland EKBB05/06) and of the Hannover Medical School, Germany (2699-2015) approved the culture of human primary lung cells. Informed consent was obtained from all subjects in the study. All mouse procedures were conducted at the Hannover Medical School, Germany in accordance with the German law for animal protection and the European Directive 2010/63/EU and were approved by the Lower Saxony State Office for Consumer Protection and Food Safety in Oldenburg/Germany (LAVES); AZ: 33.12-42502-04-15/1896 and AZ: 33.19-42502-04-15/2017), AZ:33.12-42502-04-17/2612).

Consent for publication

Not applicable.

Competing interests

The authors declare that they have no competing interests.

Author details

[1]Department of Biomedicine and Clinics of Respiratory Medicine, University Hospital Basel, University of Basel, Hebelstrasse 20, 4031 Basel, Switzerland. [2]Fraunhofer Institute for Toxicology and Experimental Medicine, 30625 Hannover, Germany. [3]Department of Pulmonology and Infectious Diseases, Hannover Medical School, Hannover, Germany. [4]Institute of Medical Genetics and Pathology, University Hospital Basel, University of Basel, 4031 Basel, Switzerland. [5]Institute of Functional and Applied Anatomy, Hannover Medical School, 30625 Hannover, Germany. [6]Institute of Pathology, Medical Faculty, RWTH University Aachen, 52074 Aachen, Germany. [7]Biomedical Research in Endstage and Obstructive Lung Disease Hannover (BREATH), Member of the German Center for Lung Research (DZL), 30625 Hannover, Germany.

References

1. Raghu G, Collard HR, Egan JJ, Martinez FJ, Behr J, Brown KK, Colby TV, Cordier JF, Flaherty KR, Lasky JA, Lynch DA, Ryu JH, Swigris JJ, Wells AU, Ancochea J, Bouros D, Carvalho C, Costabel U, Ebina M, Hansell DM, Johkoh T, Kim DS, King TE Jr, Kondoh Y, Myers J, Muller NL, Nicholson AG, Richeldi L, Selman M, Dudden RF, Griss BS, Protzko SL, Schunemann HJ. An official ATS/ERS/JRS/ALAT statement: idiopathic pulmonary fibrosis: evidence-based guidelines for diagnosis and management. Am J Respir Crit Care Med. 2011;183:788–824.
2. Selman M, King TE, Pardo A. Idiopathic pulmonary fibrosis: prevailing and evolving hypotheses about its pathogenesis and implications for therapy. Ann Intern Med. 2001;134:136–51.
3. Barkauskas CE, Cronce MJ, Rackley CR, Bowie EJ, Keene DR, Stripp BR, Randell SH, Noble PW, Hogan BL. Type 2 alveolar cells are stem cells in adult lung. J Clin Investig. 2013;123:3025–36.
4. Prasse A, Binder H, Schupp JC, Kayser G, Bargagli E, Jaeger B, Hess M, Rittinghausen S, Vuga L, Lynn H, Violette S, Jung B, Quast K, Vanauden-aerde B, Xu Y, Hohlfeld JM, Krug N, Herazo-Maya JD, Rottoli P, Wuyts WA, Kaminski N. BAL cell gene expression is indicative of outcome and airway basal cell involvement in idiopathic pulmonary fibrosis. Am J Respir Crit Care Med. 2019;199:622–30.
5. Seibold MA, Smith RW, Urbanek C, Groshong SD, Cosgrove GP, Brown KK, Schwarz MI, Schwartz DA, Reynolds SD. The idiopathic pulmonary fibrosis honeycomb cyst contains a mucociliary pseudostratified epithelium. PLoS ONE. 2013;8: e58658.
6. Khan P, Fytianos K, Blumer S, Roux J, Gazdhar A, Savic S, Knudsen L, Jonigk D, Kuehnel MP, Mykoniati S, Tamm M, Geiser T, Hostettler KE. Basal-like cell-conditioned medium exerts anti-fibrotic effects in vitro and in vivo. Front Bioeng Biotechnol. 2022;10: 844119.
7. Plantier L, Crestani B, Wert SE, Dehoux M, Zweytick B, Guenther A, Whitsett JA. Ectopic respiratory epithelial cell differentiation in bronchiolised distal airspaces in idiopathic pulmonary fibrosis. Thorax. 2011;66:651–7.
8. Chilosi M, Poletti V, Murer B, Lestani M, Cancellieri A, Montagna L, Piccoli P, Cangi G, Semenzato G, Doglioni C. Abnormal re-epithelialization and lung remodeling in idiopathic pulmonary fibrosis: the role of deltaN-p63. Lab Investig J Tech Methods Pathol. 2002;82:1335–45.
9. Smirnova NF, Schamberger AC, Nayakanti S, Hatz R, Behr J, Eickelberg O. Detection and quantification of epithelial progenitor cell populations in human healthy and IPF lungs. Respir Res. 2016;17:83.
10. Hostettler KE, Gazdhar A, Khan P, Savic S, Tamo L, Lardinois D, Roth M, Tamm M, Geiser T. Multipotent mesenchymal stem cells in lung fibrosis. PLoS ONE. 2017;12: e0181946.
11. Khan P, Roux J, Blumer S, Knudsen L, Jonigk D, Kuehnel MP, Tamm M, Hostettler KE. Alveolar basal cells differentiate towards secretory epithelial- and aberrant basaloid-like cells in vitro. Cells. 2022;11:1820.
12. Raghu G, Remy-Jardin M, Myers JL, Richeldi L, Ryerson CJ, Lederer DJ, Behr J, Cottin V, Danoff SK, Morell F, Flaherty KR, Wells A, Martinez FJ, Azuma A, Bice TJ, Bouros D, Brown KK, Collard HR, Duggal A, Galvin L, Inoue Y, Jenkins RG, Johkoh T, Kazerooni EA, Kitaichi M, Knight SL, Mansour G, Nicholson AG, Pipavath SNJ, Buendía-Roldán I, Selman M, Travis WD, Walsh SLF, Wilson KC. Diagnosis of idiopathic pulmonary fibrosis an official ATS/ERS/JRS/ALAT clinical practice guideline. Am J Respir Crit Care Med. 2018;198:e44–68.
13. Seidel P, Merfort I, Hughes JM, Oliver BG, Tamm M, Roth M. Dimethylfumarate inhibits NF-{kappa}B function at multiple levels to limit airway smooth muscle cell cytokine secretion. Am J Physiol Lung Cell Mol Physiol. 2009;297:L326-339.
14. Bankhead P, Loughrey MB, Fernández JA, Dombrowski Y, McArt DG, Dunne PD, McQuaid S, Gray RT, Murray LJ, Coleman HG, James JA, Salto-Tellez M, Hamilton PW. QuPath: Open source software for digital pathology image analysis. Sci Rep. 2017;7:16878.
15. Schmidt U, Weigert M, Broaddus C, Myers G. Cell Detection with Starconvex Polygons. [serial online] 2018 [cited June 01, 2018]. Available from: https://ui.adsabs.harvard.edu/abs/2018arXiv180603535S.
16. Jacob A, Vedaie M, Roberts DA, Thomas DC, Villacorta-Martin C, Alysandratos K-D, Hawkins F, Kotton DN. Derivation of self-renewing lung alveolar epithelial type II cells from human pluripotent stem cells. Nat Protoc. 2019;14:3303–32.
17. Schindelin J, Arganda-Carreras I, Frise E, Kaynig V, Longair M, Pietzsch T, Preibisch S, Rueden C, Saalfeld S, Schmid B, Tinevez JY, White DJ, Hartenstein V, Eliceiri K, Tomancak P, Cardona A. Fiji: an open-source platform for biological-image analysis. Nat Methods. 2012;9:676–82.
18. Suarez-Arnedo A, Torres Figueroa F, Clavijo C, Arbeláez P, Cruz JC, Muñoz-Camargo C. An image J plugin for the high throughput image analysis of in vitro scratch wound healing assays. PLoS ONE. 2020;15: e0232565.
19. Jaeger B, Schupp JC, Plappert L, Terwolbeck O, Artysh N, Kayser G, Engelhard P, Adams TS, Zweigerdt R, Kempf H, Lienenklaus S, Garrels W, Nazarenko I, Jonigk D, Wygrecka M, Klatt D, Schambach A, Kaminski N, Prasse A. Airway basal cells show a dedifferentiated KRT17highPhenotype and promote fibrosis in idiopathic pulmonary fibrosis. Nat Commun. 2022;13:5637.
20. Rosas IO, Richards TJ, Konishi K, Zhang Y, Gibson K, Lokshin AE, Lindell KO, Cisneros J, Macdonald SD, Pardo A, Sciurba F, Dauber J, Selman M, Gochuico BR, Kaminski N. MMP1 and MMP7 as potential peripheral blood biomarkers in idiopathic pulmonary fibrosis. PLoS Med. 2008;5: e93.
21. Adams TS, Schupp JC, Poli S, Ayaub EA, Neumark N, Ahangari F, Chu SG, Raby BA, Deluliis G, Januszyk M, Duan Q, Arnett HA, Siddiqui A, Washko GR, Homer R, Yan X, Rosas IO, Kaminski N. Single-cell RNA-seq reveals ectopic and aberrant lung-resident cell populations in idiopathic pulmonary fibrosis. Sci Adv. 2020;6: eaba1983.

Blumer *et al. Respiratory Research*   (2024) 25:26

Page 14 of 14

22. Habermann AC, Gutierrez AJ, Bui LT, Yahn SL, Winters NI, Calvi CL, Peter L, Chung M-I, Taylor CJ, Jetter C, Raju L, Roberson J, Ding G, Wood L, Sucre JMS, Richmond BW, Serezani AP, McDonnell WJ, Mallal SB, Bacchetta MJ, Loyd JE, Shaver CM, Ware LB, Bremner R, Walia R, Blackwell TS, Banovich NE, Kropski JA. Single-cell RNA sequencing reveals profibrotic roles of distinct epithelial and mesenchymal lineages in pulmonary fibrosis. Sci Adv. 2020;6: eaba1972.

23. Kathiriya JJ, Wang C, Zhou M, Brumwell A, Cassandras M, Le Saux CJ, Cohen M, Alysandratos K-D, Wang B, Wolters P, Matthay M, Kotton DN, Chapman HA, Peng T. Human alveolar type 2 epithelium transdifferentiates into metaplastic KRT5+ basal cells. Nat Cell Biol. 2022;24:10–23.

24. Reyfman PA, Walter JM, Joshi N, Anekalla KR, McQuattie-Pimentel AC, Chiu S, Fernandez R, Akbarpour M, Chen CI, Ren Z, Verma R, Abdala-Valencia H, Nam K, Chi M, Han S, Gonzalez-Gonzalez FJ, Soberanes S, Watanabe S, Williams KJN, Flozak AS, Nicholson TT, Morgan VK, Winter DR, Hinchcliff M, Hrusch CL, Guzy RD, Bonham CA, Sperling AI, Bag R, Hamanaka RB, Mutlu GM, Yeldandi AV, Marshall SA, Shilatifard A, Amaral LAN, Perlman H, Sznajder JI, Argento AC, Gillespie CT, Dematte J, Jain M, Singer BD, Ridge KM, Lam AP, Bharat A, Bhorade SM, Gottardi CJ, Budinger GRS, Misharin AV. Single-cell transcriptomic analysis of human lung provides insights into the pathobiology of pulmonary fibrosis. Am J Respir Crit Care Med. 2019;199:1517–36.

25. Strunz M, Simon LM, Ansari M, Kathiriya JJ, Angelidis I, Mayr CH, Tsidiridis G, Lange M, Mattner LF, Yee M, Ogar P, Sengupta A, Kukhtevich I, Schneider R, Zhao Z, Voss C, Stoeger T, Neumann JHL, Hilgendorff A, Behr J, O'Reilly M, Lehmann M, Burgstaller G, Königshoff M, Chapman HA, Theis FJ, Schiller HB. Alveolar regeneration through a Krt8+ transitional stem cell state that persists in human lung fibrosis. Nat Commun. 2020;11:3559.

26. Xu Y, Mizuno T, Sridharan A, Du Y, Guo M, Tang J, Wikenheiser-Brokamp KA, Perl A-KT, Funari VA, Gokey JJ, Stripp BR, Whitsett JA. Single-cell RNA sequencing identifies diverse roles of epithelial cells in idiopathic pulmonary fibrosis. JCI Insight 2017; 1.

27. Fernanda de Mello Costa M, Weiner AI, Vaughan AE. Basal-like progenitor cells: a review of dysplastic alveolar regeneration and remodeling in lung repair. Stem Cell Rep. 2020;15:1015–25.

28. Kumar PA, Hu Y, Yamamoto Y, Hoe NB, Wei TS, Mu D, Sun Y, Joo LS, Dagher R, Zielonka EM, Wang DY, Lim B, Chow VT, Crum CP, Xian W, McKeon F. Distal airway stem cells yield alveoli in vitro and during lung regeneration following H1N1 influenza infection. Cell. 2011;147:525–38.

29. Yuan T, Volckaert T, Redente EF, Hopkins S, Klinkhammer K, Wasnick R, Chao CM, Yuan J, Zhang JS, Yao C, Majka S, Stripp BR, Günther A, Riches DWH, Bellusci S, Thannickal VJ, De Langhe SP. FGF10-FGFR2B signaling generates basal cells and drives alveolar epithelial regeneration by bronchial epithelial stem cells after lung injury. Stem cell reports. 2019;12:1041–55.

30. Martin WR, Brown C, Zhang YJ, Wu R. Growth and differentiation of primary tracheal epithelial cells in culture: regulation by extracellular calcium. J Cell Physiol. 1991;147:138–48.

31. Zhang C, Lee HJ, Shrivastava A, Wang R, McQuiston TJ, Challberg SS, Pollok BA, Wang T. Long-term in vitro expansion of epithelial stem cells enabled by pharmacological inhibition of PAK1-ROCK-myosin II and TGF-β signaling. Cell Rep. 2018;25:598-610.e595.

32. Zuo F, Kaminski N, Eugui E, Allard J, Yakhini Z, Ben-Dor A, Lollini L, Morris D, Kim Y, DeLustro B, Sheppard D, Pardo A, Selman M, Heller RA. Gene expression analysis reveals matrilysin as a key regulator of pulmonary fibrosis in mice and humans. Proc Natl Acad Sci USA. 2002;99:6292–7.

33. Selman M, Pardo A, Barrera L, Estrada A, Watson SR, Wilson K, Aziz N, Kaminski N, Zlotnik A. Gene expression profiles distinguish idiopathic pulmonary fibrosis from hypersensitivity pneumonitis. Am J Respir Crit Care Med. 2006;173:188–98.

34. Levardon H, Yonker LM, Hurley BP, Mou H. Expansion of airway basal cells and generation of polarized epithelium. Bio Protoc. 2018; 8.

35. Gerovac BJ, Valencia M, Baumlin N, Salathe M, Conner GE, Fregien NL. Submersion and hypoxia inhibit ciliated cell differentiation in a notch-dependent manner. Am J Respir Cell Mol Biol. 2014;51:516–25.

36. Boesch M, Baty F, Brutsche MH, Tamm M, Roux J, Knudsen L, Gazdhar A, Geiser T, Khan P, Hostettler KE. Transcriptomic profiling reveals disease-specific characteristics of epithelial cells in idiopathic pulmonary fibrosis. Respir Res. 2020;21:165.

37. Chen H, Matsumoto K, Brockway BL, Rackley CR, Liang J, Lee JH, Jiang D, Noble PW, Randell SH, Kim CF, Stripp BR. Airway epithelial progenitors are region specific and show differential responses to bleomycin-induced lung injury. Stem cells (Dayton, Ohio). 2012;30:1948–60.

Publisher's Note